

OBSERVATIONS OF FLUX JUMP BEHAVIOR RELATED TO VARIOUS CHANGES
OF GEOMETRY, AND THERMAL AND ELECTRICAL ENVIRONMENT*

A.D. McInturff
Brookhaven National Laboratory
Upton, New York

These observations were made in the process of measuring hysteresis curves for Nb₃Sn ribbons, and TiNb ribbons, wires, and composites. The term flux jump stability for the duration of this paper will be in reference to the frequency or number, and the magnitude [percentage of $\bar{M}(H_a)$ changed during a flux jump only] of the flux jumps as they occur in the magnetization curves. The term thermal environment will refer to the helium bath or vapor temperature and also whether the sample is thermally insulated from or is well ventilated with that bath or vapor. The term electrical environment refers to the effects of $\partial H/\partial t$, the probability of flux jumping at a given (H) field, external transport current effects on the flux jump behavior, field reversal effects on the flux jump behavior, and the conductivity (electrical and/or thermal) of the normal metal matrix surrounding the superconductor. The geometry changes, which were made in the study of flux jump behavior, were changes in sample dimensions, in the angle of the sample with respect to the magnetic field, and in the magnetic field-transport current geometry.

The experimental setup (similar to that of Fietz¹) consisted of various carefully matched (≤ 1 turn in 10^4) coil pairs, one pair for each geometry to be investigated. Several variations from infinite sheet to thin disk were investigated, with or without transport current (see Fig. 1). One coil was used to measure $\partial \bar{H}(\text{helium} + \text{sample})/\partial t$, the other to measure $\partial \bar{H}(\text{helium})/\partial t$. The difference signal from these coils was integrated, employing a chopper-stabilized operational amplifier, and was displayed on the y-axis of an x-y recorder. The signal from the $\partial \bar{H}(\text{helium})/\partial t$ coil was integrated similarly and displayed on the x-axis of the recorder. The time constant for the magnetization \bar{M} integrator (difference signal) was 0.01 to 0.05 sec.

The sample was placed in the specimen coil and the magnetic field was cycled either from $H = 0 \rightarrow H_{\max} \rightarrow H = 0$, or $\rightarrow -H_{\max}$. The resulting hysteresis curve was simultaneously plotted on the x-y recorder. When transport current was employed only two of the sequences mentioned by LeBlanc² were used. First the transport current was raised to some predetermined value and then the field was cycled, or alternatively the field (H) was cycled to a given magnitude and then the transport current was applied until the superconducting sample became resistive. The latter sequence was performed on both the diamagnetic and paramagnetic portions of the magnetization curves \bar{M} .

The thermal dependence of the flux jumps can most dramatically be seen in Fig. 2. The dramatic increase in flux jumps at lower temperatures had previously been reported by several investigators.³⁻⁸ This thermal effect can be generalized by the following statement: a decrease in temperature will increase the frequency, but reduce the magnitude of the individual flux jumps. The reduction in magnitude shown in Fig. 2b can probably be attributed to the fact that these results are obtained below the λ point of helium, where the tremendous increase in thermal conductivity of the bath made possible a more efficient transfer of heat away from the sample. This more efficient transfer of heat would restrict the amount of sample that would be heated during the flux jump.

* Work performed under the auspices of the U.S. Atomic Energy Commission.

The frequency of the flux jumps seems to increase as $\partial\bar{H}/\partial t$ is increased from a few gauss/minute to several hundred gauss/minute. Once the rate has reached several kilogauss/minute, the flux jumps seem (given all other parameters the same) to have almost identical characteristics. The flux jumps observed seem to be more frequent at fields less than or equal to \bar{H}^* (\bar{H}^* = the magnetic field necessary for complete penetration) and in some cases slightly greater than \bar{H}^* . The exceptions to this observation were in those cases where a transport current equal to a significant percentage of the critical transport current was present. Then the flux jumps would occur even at fields several times greater than \bar{H}^* . These flux jumps would almost always result in the samples becoming resistive. This might be explained if one notes that in these experiments the current and magnetic field were perpendicular. Therefore, due to this geometry, a large Lorentz force could have caused physical motion.

The effect of magnetic field reversal greatly increased the flux jump instability, as is illustrated in Fig. 3c vs Fig. 3d. This phenomenon can be understood from arguments presented by Schweitzer and the author⁹ in a paper on flux mobility recently submitted for publication.

The configuration of a thin plate [e.g., 1 cm wide ribbon (Nb₃Sn or TiNb) with \bar{H} perpendicular to the large flat surface] is, usually for the commercially available type II superconductors, flux jump unstable. Figures 3 and 4 show a typical geometry dependence of the magnetization of a thin plate as a function of the minimum width dimension of the superconductor. Figures 5 and 6 show the effect of high conductivity metal bonded to the type II superconductors Nb₃Sn and TiNb. This effect can probably be attributed to the thermal conductivity in that these samples were edge-cooled stacks. Future experiments will be necessary to validate the above remark.

Some early results seem to indicate that scribing the normal metal reduces the flux jump instability. But the corresponding reduction in magnetization and flux jump instability that was reported for the Nb₃Sn sample did not seem to be valid for the TiNb samples. It should be noted that these data are very crude measurements and future experimentation will be necessary to validate them.

There was a coupling effect on the magnetization and flux jump stability observed in the process of these measurements. If a sample stack is prepared with no electrical insulators between layer or ribbon samples, the magnetization rises to much greater values and the severity of the flux jumps greatly increases as well. (This is easily understood by the flux jump stability criteria put forth by various workers in the field.¹⁰⁻¹⁴) If the samples were electrically (and thermally) insulated the frequency of the flux jumps was greatly increased.

In conclusion it would seem to the author that the aforementioned data present a favorable case for multifilament conductor contained in a high conductivity (thermal) matrix. From arguments presented by P.F. Smith¹⁵ one would also conclude that a low electrical conductivity interface between the superconductor and the matrix to prevent possible coupling is required.

These data were taken to compare with pulsed coil data¹⁶ for loss rate determination. The values used for comparison were taken to be those that would have been present if the flux jumps had not occurred. These results seem to check fairly consistently if one takes into account the diamagnetic effects of the superconductors on the field as calculated for copper windings.

The author expresses his sincere thanks to P.F. Dahl for his corrections to and suggestions for this paper and to W.B. Sampson and R.B. Britton for the use of their magnets in these experiments.

REFERENCES

1. W.A. Fietz, Rev. Sci. Instr. 36, 1621 (1965).
2. M.A.R. LeBlanc, Phys. Rev. Letters 11, 149 (1963); M.A.R. LeBlanc, Phys. Rev. Letters 6, 140 (1963); M.A.R. LeBlanc et al., Phys. Rev. Letters 14, 704 (1965).
3. Y.B. Kim et al., Phys. Rev. 131, 2486 (1963).
4. G. Kuhn et al., Compt. Rend. Paris 255, 2923 (1962).
5. R.D. Blangher et al., Cleveland Conference on Superconductivity, 4, p. 121 (1968).
6. L.J. Neuringer et al., Phys. Rev. 148, 231 (1966).
7. J.M.P. Watson, J. Appl. Phys. 37, 516 (1966).
8. M.R. Wertheimer et al., J. Phys. Chem. Solids 28, 2509 (1967).
9. D.G. Schweitzer and A.D. McInturff, to be published.
10. R. Hancox, private communication.
11. S.L. Wipf, these Proceedings, p. 511.
12. H.R. Hart, Jr., *ibid.*, p. 571.
13. P.F. Smith, *ibid.*, p. 839.
14. Z.J.J. Stekly, *ibid.*, p. 748.
15. P.F. Smith, *ibid.*, p. 913.
16. G.H. Morgan, P.F. Dahl, W.B. Sampson, and R.B. Britton, to be published.

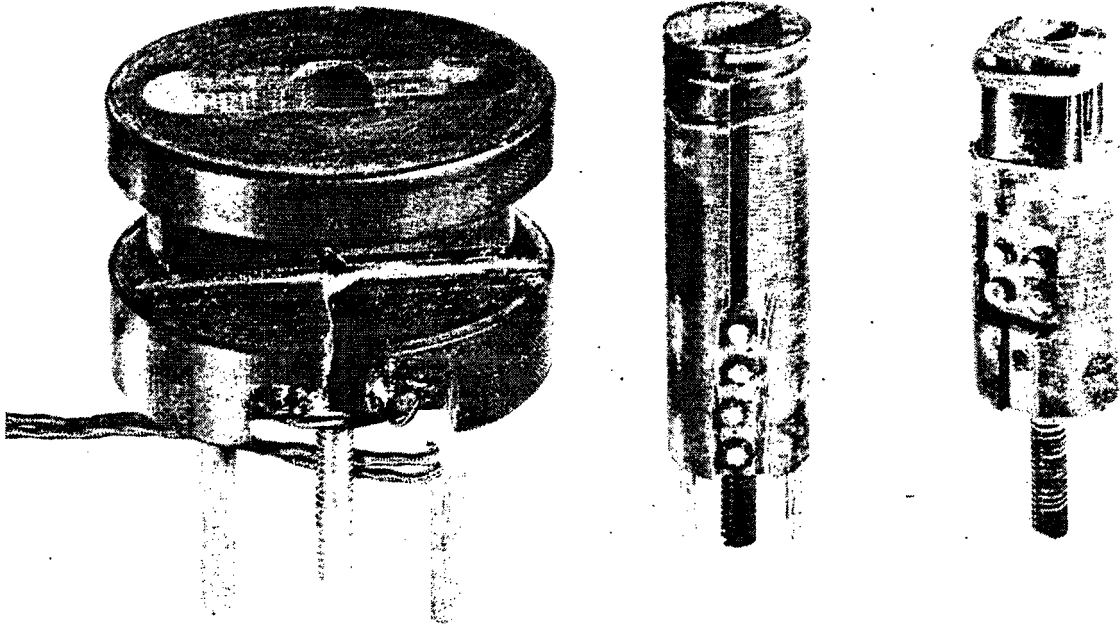


Fig. 1. Three of the coil pairs used in the experiments. The coils on the left are for thin disk and perpendicular transport current (5×10^3 turns each of No. 50 wire). The middle coils are thin disk coils (for stacks) (10^4 turns each of No. 50 wire). The coil pair on the right are for the infinite sheet geometry (2×10^4 turns each of No. 50 wire).

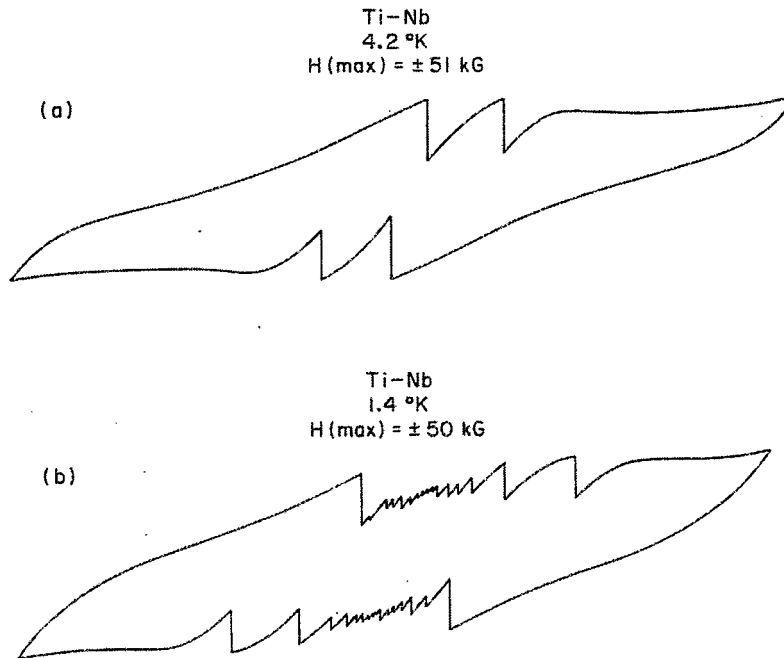


Fig. 2. Tracings of an x-y recorder of \bar{M} vs H for Ti48a/oNb at 4.2°K. and below the λ point 1.4°K. These tracings are for the same sample.

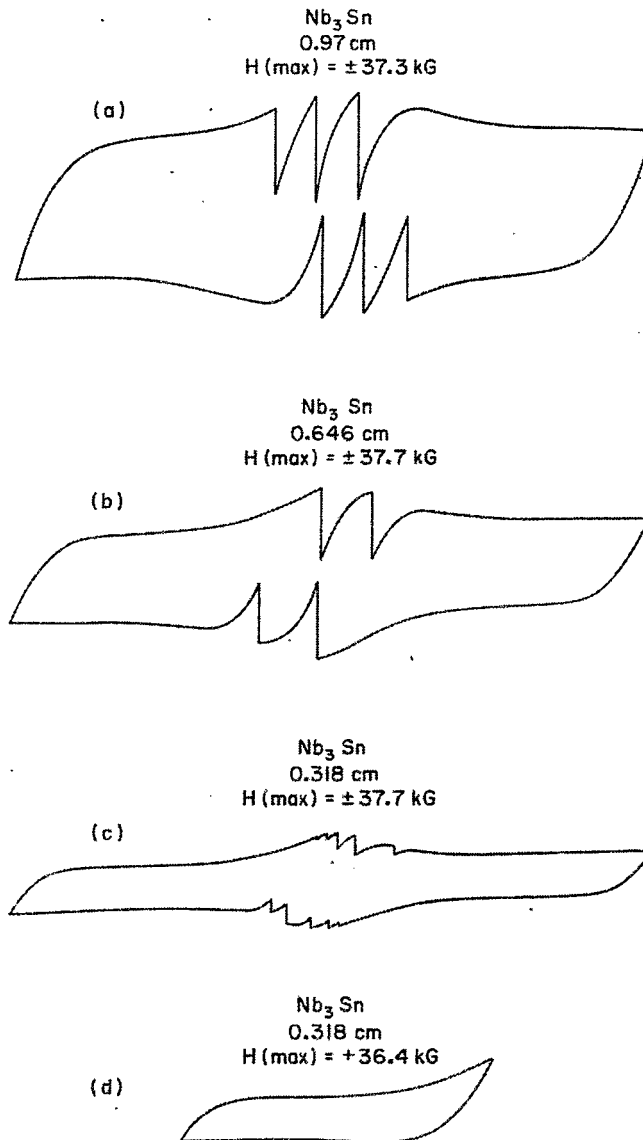


Fig. 3. Tracings (a sample of vapor-deposited Nb_3Sn) of an x-y recorder with \bar{M} as the y-input and H as the x-input. Curves 3a, b, and c are for both senses of \bar{M} (plus H_{max} and minus H_{max}). Curve 3d is for the plus H_{max} only.

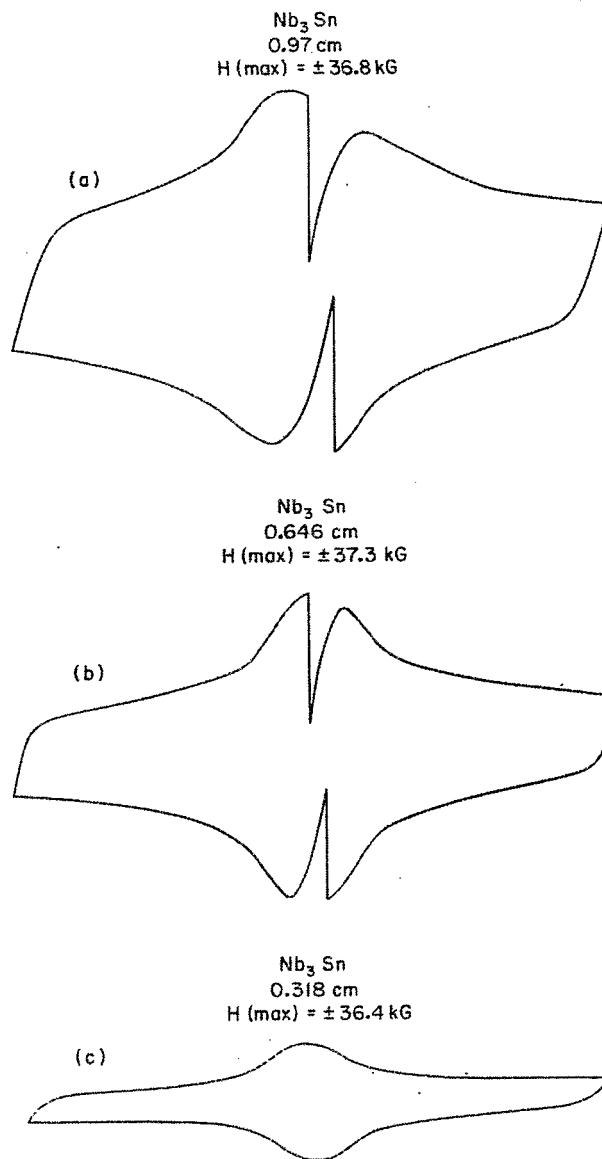
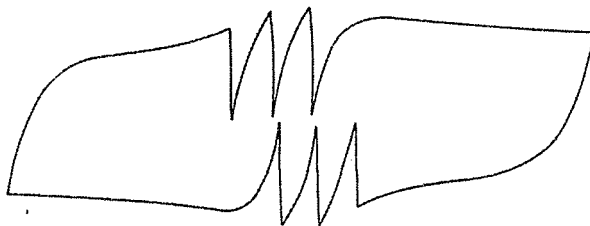


Fig. 4. Tracings of an x-y recorder (a sample of diffusion processed Nb_3Sn); y-axis is \bar{M} and x-axis is \bar{H} . These curves are for the same sample, only varying the width of the ribbon (but not the amount).

Nb₃Sn

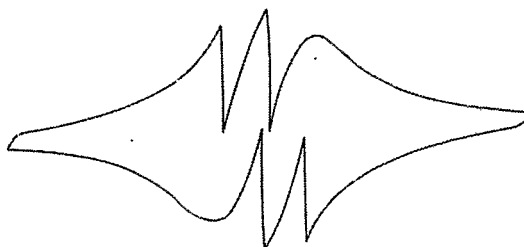


Nb₃Sn



Fig. 5. Tracings of an x-y recorder (Nb₃Sn); y-axis is \bar{M} and x-axis is \bar{H} . The upper curve is taken with the Ag plating in good contact; in the lower curve that contact is broken. $H_{\max} = \pm 50$ kG. This is a thin disk configuration (1 cm x 1 cm).

Ti-Nb



Ti-Nb

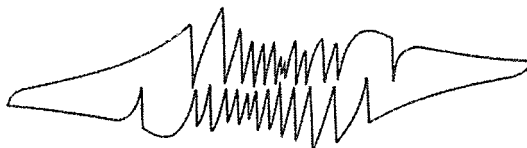


Fig. 6. Tracings of an x-y recorder for \bar{M} as the y-axis and \bar{H} on the x-axis ($H_{\max} = \pm 40$ kG). The upper curve is for a Ti48a/oNb sample with an excellent Cu to TiNb bond; in the lower curve the bond was highly resistive. This is for a thin disk configuration (1 cm x 1 cm).